agronomy

MDPI

Article

A Deep Learning Model of Radio Wave Propagation for Precision Agriculture and Sensor System in Greenhouses

Dora Cama-Pinto [1], Miguel Damas [1], Juan Antonio Holgado-Terriza [2], Francisco Manuel Arrabal-Campos [3,4], Juan Antonio Martínez-Lao [3], Alejandro Cama-Pinto [5] and Francisco Manzano-Agugliaro [3,4,*]

1 Department of Computer Architecture and Technology, University of Granada, 18071 Granada, Spain
2 Software Engineering Department, University of Granada, 18071 Granada, Spain
3 Department Engineering, University of Almeria, Carretera Sacramento, s/n, La Cañada de San Urbano, 04120 Almería, Spain
4 CIAIMBITAL Research Center, CeiA3, University of Almería, Carretera Sacramento s/n, 04120 Almería, Spain
5 Faculty of Engineering, Universidad de la Costa, Calle 58 # 55-66, Barranquilla 080002, Colombia
* Correspondence: fmanzano@ual.es

Abstract: The production of crops in greenhouses will ensure the demand for food for the world's population in the coming decades. Precision agriculture is an important tool for this purpose, supported among other things, by the technology of wireless sensor networks (WSN) in the monitoring of agronomic parameters. Therefore, prior planning of the deployment of WSN nodes is relevant because their coverage decreases when the radio waves are attenuated by the foliage of the plantation. In that sense, the method proposed in this study applies Deep Learning to develop an empirical model of radio wave attenuation when it crosses vegetation that includes height and distance between the transceivers of the WSN nodes. The model quality is expressed via the parameters cross-validation, R^2 of 0.966, while its generalized error is 0.920 verifying the reliability of the empirical model.

Keywords: deep learning; neural network; precision agriculture; propagation model; wireless sensor networks

Citation: Cama-Pinto, D.; Damas, M.; Holgado-Terriza, J.A.; Arrabal-Campos, F.M.; Martínez-Lao, J.A.; Cama-Pinto, A.; Manzano-Agugliaro, F. A Deep Learning Model of Radio Wave Propagation for Precision Agriculture and Sensor System in Greenhouses. *Agronomy* **2023**, *13*, 244. https://doi.org/10.3390/agronomy13010244

Academic Editor: Roberto Marani

Received: 1 November 2022
Revised: 9 January 2023
Accepted: 10 January 2023
Published: 13 January 2023

1. Introduction

The increase in demand for crops and food production is associated with the growth of the world population, which according to data from the Food and Agriculture Organization (FAO) of the United Nations, is currently 7.7 billion humans, projected to be 9.4 billion in 2030 and 10.1 billion in 2050, when the world population will need 70% more food, 42% more arable land and 120% more water for food-related purposes [1–4]. Since traditional outdoor agriculture does not satisfy food production, coupled with the reduction of limited agricultural land for civil works construction, an optimal solution is protected crops called greenhouses that increase the number of harvests. Better yet, when transformed to smart greenhouses using information technology and sensors, can contribute to the increase of agricultural production [5].

In relation to the technological advances of Industry 4.0, cloud computing and the IoT (Internet of Things) contribute to making traditional systems smart [6–8]. An example of this process is smart farming (SF) that improves productivity and reduces surplus elements used in crops [9]. On the other hand, within the IoT concept, the role of wireless sensor networks (WSN) is paramount [10,11] because several IoT applications are based on wireless data transmission allowing sensor/actuator nodes to communicate with each other through a wireless network connection, even potentialized within the mMTC (massive machine-type communications) scenario of 5G [12–15].

Its sensors record variable data in crop fields and transfer it wirelessly to the base station for agricultural decision-making and monitoring [16]. Proper planning of the

arrangement of the number of wireless nodes within a greenhouse is a major challenge. Maximum coverage in wireless communication is a research objective to establish a model to determine the attenuation curves of the radio signal when deployed inside the greenhouse.

Several empirical models, such as Weissbeerger's or ITU-R's model for radiowave attenuation, have significant error rates when compared to results obtained in greenhouse field tests because they ignore the antenna height variable in their equations [17,18]. Efforts have been made to improve the predictions through novel models that introduce variable antenna height because foliage in crops has a different density at different spans. Among these, we highlight some that employ linear and polynomial [19–21] regressions. However, the best prediction was performed by regularized non-linear regression in [22].

There are several reasons why deep learning models may be useful, even in cases where there is a small amount of data available. First, deep learning models are particularly well-suited for tasks that involve learning from complex high-dimensional data. These types of tasks can be challenging to model using traditional machine learning approaches, but deep learning models are able to learn useful features and patterns directly from the data. Second, deep learning models are able to learn hierarchical representations of the data, with different layers of the model learning to represent different levels of abstraction. This allows the model to learn complex relationships in the data and make more accurate predictions. Third, deep learning models are able to handle large amounts of noise and variability in the data, which can be especially useful in real-world applications where data is often messy and incomplete.

This research aims to improve prediction by means of deep learning, a sub-field of machine learning, a branch of artificial intelligence, to find a new empirical model of attenuation and contrast it with the previous model (regularised regression) to determine whether it offers greater accuracy in its prediction. Until now, with respect to the literature reviewed, we found that this is the first time that, using deep learning, an empirical propagation model has been developed for application to any greenhouse plantation.

2. Background

Based on the paradigms of Industry 4.0 (Fourth Industrial Revolution), the PA (Precision Agriculture, Third Agricultural Revolution) evolved into Agriculture 4.0 (A4.0) and is also called smart farming (SF) [23]. It integrates information and communication technologies (ICT) into traditional farming practices to monitor a wide range of agricultural parameters that improve crop yields [24]. Both terms (SF and A4.0) related to digital agriculture (DA) are driving change in revolution, sustainability, efficiency, productivity, and food security. This novel paradigm is based on technologies such as IoT, artificial intelligence, big data, cloud computing, and other related smart systems and devices for crop and farm management [25–27].

Within this technological scenario, the wireless sensor networks (WSN) provide a local crop monitoring system that enables appropriate decisions to be made in a controlled production system affected by climate change [28,29]. Through wireless data transmission, WSN supports the collection of information in agriculture due to their low cost, minimal power consumption, self-organizing capability, wide area coverage by multi-hop links, and deployment in environments changed by plant growth, with limited power grid [27], contributing to improved agricultural productivity in an environmentally sustainable way [30,31]. The types of sensors for agriculture are set according to the characteristics of each plantation [32,33].

The Received Signal Strength Indicator (RSSI) reveals power values in radio wave propagation. The environment, crop growth, and antenna heights determine RSSI values [34,35]. The models used to predict the RSSI between two transceivers are called propagation models [36].

The Friis model of free space propagation was used to obtain the line-of-sight (LOS) path loss incurred in a free space environment from a transmitter to a receiver, as a relation

between the received power to the transmitted power, in terms of effective areas of the receiving (R_x) and transmitting (T_x) antenna through free space [37–44].

In greenhouses, the effects of the vegetation impact in the radio-wave propagation, which occurs with NLOS (non-line of sight). Signals at microwave (1–30 GHz) [45] and millimeter (30–300 GHz) frequencies [14] experience scattering and absorption caused by randomly distributed vegetation leaves and branches [46]. The total path losses are formulated by combining the PL_{fs} model losses with the PL_{veg} vegetation losses predicted by the different vegetation models [19,47,48].

The second category, the empirical model of path loss, was chosen for the present study because of the simplicity with which its equations are formulated, notably those listed in [21,22] based on the EDM (exponential decay model). However, its estimates have a considerable margin of error compared to those taken in field tests prompting us to focus our work to improve them.

Among empirical models, the authors developed an empirical multi-parametric equation model based on non-linear regularised regressions using experimental measurements of the RSSI signal obtained from field test measurements of four greenhouses. In that study, the evaluation of the model with 5th degree polynomials yielded 0.948 for R^2, 0.946 in R^2_{adj} (20-parameter solution), and 0.942 for R^2, y 0.940 en R^2_{adj} when the equation was reduced to 15 parameters by applying cross-validation [22].

The attenuation of the radio wave inside the greenhouse depends on the signal frequency, antenna height, and distance between antennas, exhibiting a non-linearity behavior. Therefore, an interesting approach can also be applied, taking advantage of machine learning (ML) [49] in order to find the relationship between these non-independent variables. ML builds a model automatically by deducing meaningful ideas (known as features) from the dataset, with feature extraction being the most critical step in a model generation [50]. Then the non-linear features of the input data establish interactions and relationships with the output predictor variables [51]. Analogously, humans use a model of the world as a simulator in our brain, which is obtained by learning from large amounts of data collected by our senses interacting with the surrounding environment [52].

ML collects input and output data to subsequently predict future values [53–55]. For the implementation of machine learning algorithms ANNs (artificial neural networks) [56–60]. Based on this architecture, ANNs can be classified into CNNs (convolutional neural networks) [61–63] and recurrent neural networks (RNNs) [62,64].

DL (Deep learning) is a form or subfield of ML [65,66]. ANNs are the core algorithms of DL. If the depth or number of layers of the ANN is greater than three, it will cease to be a simple ANN and become a DL algorithm [67], called a deep neural network (DLL), allowing it to successfully interpret more complex non-linear inputs [68–71]. As mentioned before, although there has been no research using ML in the estimation of radio propagation loss in the presence of vegetation, there are some works related to radio propagation, such as DNN-based, employing CNN for radio propagation loss estimation using spatial information, such as building occupancy maps for input data [72], path loss prediction in rural areas using 3.7 GHz band, combines different ML models, for the base learning stage uses ANN, DT (decision trees), SVR (support vector regression), kNN (k-nearest neighbors), GLM (generalized linear model) and a custom DNN with three hidden layers as meta-learner [73]. The paper by Bogdándy et al. [74] used the log of WiFi RSSI values as input data to determine the indoor positioning of nodes with an ANN. In addition, [75] used ML to obtain an ANN-based model that predicts radio propagation loss characteristics inside tunnels.

3. Materials and Methods

3.1. Source of Data

All data were collected by Cama-Pinto et al. [21,22]. The experiment was performed in greenhouses located in Almería, southeastern Spain [76–79]. Vegetable and fruit production is exported mainly to the EU [80–87]. RSSI data are from trials in four greenhouse fields

during February 2020, each with areas of 10,000 m^2 in the Almeria localities of La Cañada, Retamar, El Alquian, Níjar, and greenhouse test data from La Cañada in 2018. The total number of data collected were 345. Each experiment was repeated 10 times in 2020 and 60 times in 2018. The data used was the average of the experiments. The outline of the measurement system hardware configuration is detailed by the authors in [88].

As shown in Figure 1, during the measurement phase, the antennas of the T_x node and the sink node (R_x) were placed at the same height. The signal arrived at the receiver attenuated after passing through the tomato plant walls (1 m thick) every 5 min, repeating the process 10 times:

(1) For the measurement, both the T_x node and the sink are located at equal distances from the ground. Every 5 min the R_x node records the signal from the T_x node, which arrives attenuated. The measurement is repeated 10 times, then the distance between the nodes is increased by adding one more tomato wall and doubling the previous procedure. After the separation increases by adding more tomato plant walls, there comes a point where there is no communication, ending this stage.

(2) The T_x and R_x nodes are moved two meters next to the tomato wall into the side corridor and step 1 is repeated.

(3) Steps 1 and 2 are followed with different heights (the heights in centimeters are 30, 50, 70, 90, 100, 150, and 200).

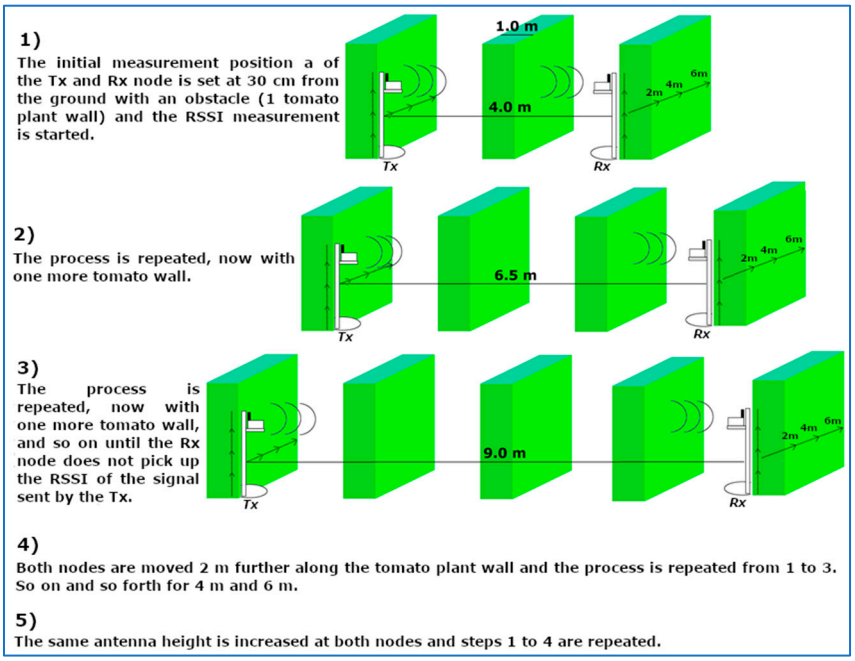

Figure 1. Location of nodes inside the greenhouse during field tests.

The schematic of the top view of the deployment of the T_x and R_x nodes inside the greenhouse is shown in Figure 2.

3.2. Evaluation of the Model's Performance

The predictive performance of the model was assessed using seven (07) criteria. The mean square error (MSE), root mean square error (RMSE), mean absolute percentage error (MAPE), coefficient of determination (R^2), adjusted coefficient of determination (R^2_{adj}), Akaike information criterion (AIC), and the Bayesian information criterion BIC, also called the Schwarz information criterion—SBC [89–98].

The accuracy or assessment of model performance can be verified by the R^2, its variant, the R^2_{adj} and Q^2 [99–105]. On the other hand, AIC and SBC are widely used for model selection [106–117].

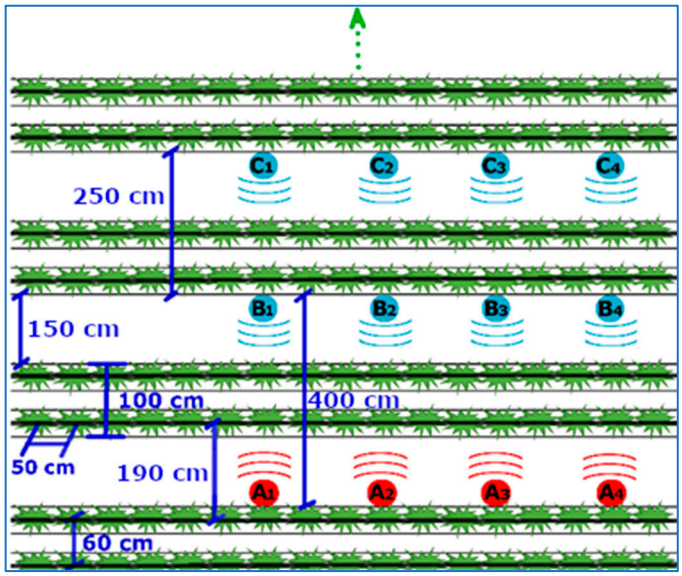

Figure 2. Top view of the deployment of the T_x and R_x nodes inside the greenhouse.

4. A Deep Learning Model of Radio Wave Propagation

A novel deep learning model is proposed in this work based on binary feedforward neural network. It is composed of two layers, an encoding and a decoding layer. The encoding layer converts the distance and the height at which the attenuation is to be known into binary. Since the range of data is limited. The number of bits to determine the integer part and the decimal part will be small. The distance varies from 1 to 35 m, and the height varies from 30 cm to 200 cm. The encoding is done using 14 bits for the distance 7 for the integer part and the other 7 for the decimal part. For height, we used 11 bits, 4 of them for the integer part and the rest for the decimal part, giving two real numbers with two decimals using 25 bits in total. The decoding converts from binary to real number with an accuracy of 3 decimal places, using 17 bits to perform this conversion to the real number, so it used 7 bits for the integer part and the other 10 for the decimal part. The neural network is composed of 7 layers. The first and the last are the input and output layers, respectively. The rest of the layers are hidden. Figure 3 below shows the structure of the deep neural network. The activation function for the perceptrons is the sigmoid function. The input layer has 25 perceptrons corresponding to the 25 input bits, while the output layer has 17 perceptrons corresponding to the 17 output bits.

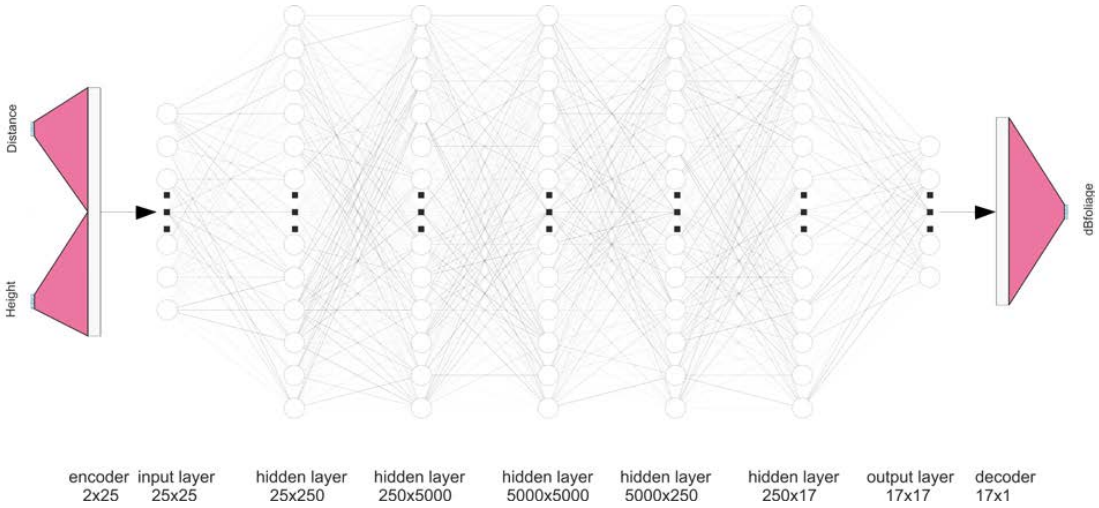

Figure 3. Schematic of the Deep Learning Model for the estimation of attenuation from distance and height.

The distance and height values compose the vector X while the estimated attenuation values $L_{foliage}(d,h)$ or measured dB are Y. The representation of the two vectors X and Y is shown in Figure 4 below,

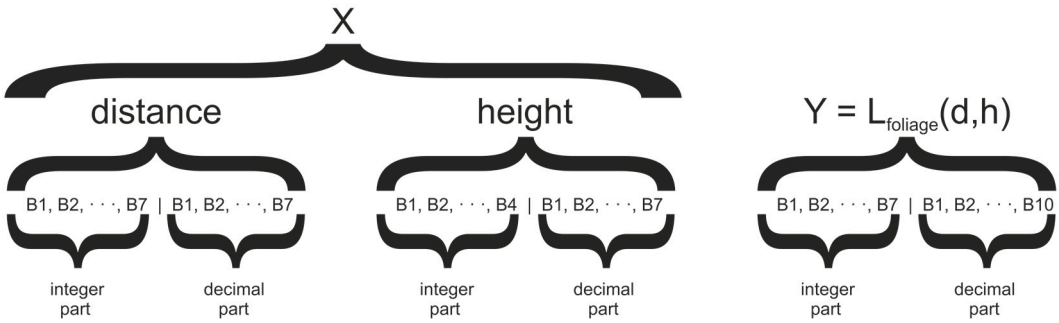

Figure 4. Representation of distance and height, which is composed the vector X, while the estimated attenuation values $L_{foliage}(d,h)$ or measured dB are composed of Y. The B values are bits that can take the values either 0 or 1. Then, for creating the real number, the distance, height, and $L_{foliage}(d,h)$ have a integer part and decimal part.

The parametric adjustment of the deep neural network is performed by minimizing the following cost function is,

$$J(\theta) = \frac{1}{m}\sum_{i=1}^{m}\sum_{k=1}^{K}\left[-y^i \log\left(h_\theta(x^i)\right) - \left(1-y^i\right)\log\left(1-h_\theta(x^i)\right)\right] \quad (1)$$

where m is the number of experiment performed in the greenhouse, where for a distance and height given, we obtain a signal attenuation, and K is the total number of bits in the output layer. The logistic function is defined as,

$$h_\theta = g\left(\theta^T x\right) \quad (2)$$

where g is the sigmoid function,

$$g(z) = \frac{1}{1+e^{-z}} \quad (3)$$

To avoid deviations and overfitting of the cost function parameters of Equation (1), the regularization function called Tikhonov regularization [118,119] is added as follows,

$$J(\theta) = \frac{1}{m}\sum_{i=1}^{m}\sum_{k=1}^{K}\left[-y^i \log\left(h_\theta(x^i)\right) - \left(1-y^i\right)\log\left(1-h_\theta(x^i)\right)\right] + \frac{\lambda}{2m}\left[\sum_{n=1}^{N-1}\sum_{j=1}^{J_n}\sum_{s=1}^{S_n}\left(\theta_{j,s}^{(n)}\right)^2\right] \quad (4)$$

The network parameters are represented by $\theta_{j,k}^{(i)}$, where N is the number of layers, J_n is the number of total incoming connections at the n-th layer, and S_n is the number of total incoming connections at the n-th layer. λ is the regularising term and establishes the weight that the parameters should have in the cost function, avoiding overfitting and variability in the parameterized functions. In this optimization problem, it is mandatory to determine the gradients in each direction. The gradients can be calculated using the backpropagation algorithm (see Algorithm 1).

Once the gradients have been calculated, the Polac–Ribiere method [120] is used to calculate the conjugate gradients to estimate the search direction. The approximation is performed using quadratic polynomial functions. The stopping criterion used is the so-called Wolfe-Powel conditions [121,122].

Algorithm 1 Backtracking Algorithm Applied in the Deep Learning

1	Training set $\left\{\left(x^{(1)}, y^{(1)}\right), \left(x^{(2)}, y^{(2)}\right), \ldots, \left(x^{(m)}, y^{(m)}\right)\right\}$
2	For the entire training package
3	It establishes $\Delta_{ij}^{(n)} = 0$
4	Compute forward propagation
5	Compute regularized cost function $J(\theta)$
6	Set $a^{(1)} = x^{(i)}$
7	Perform forward propagation to compute $a^{(n)}$ for $n = 2, 3, \ldots, N$
8	Using $y^{(i)}$, compute $\delta^{(N)} = a^{(N)} - y^{(i)}$
9	Compute $\delta^{(N-1)}, \delta^{(N-2)}, \delta^{(N-3)}, \ldots, \delta^{(2)}$
10	$\Delta_{ij}^{(n)} := \Delta_{ij}^{(n)} + a_j^n \delta_i^{(n+1)}$
11	$D_{ij}^{(l)} := \frac{1}{m}\Delta_{ij}^{(n)} + \lambda\theta_{ij}^{(n)}$ if $j \neq 0$
12	$D_{ij}^{(l)} := \frac{1}{m}\Delta_{ij}^{(n)}$ if $j = 0$
13	$\frac{\partial}{\partial\theta_{ij}^{(n)}} J(\theta) = D_{ij}^{(n)}$

The total number of parameters conditions both the training time and the density of perceptrons in the neural network. A study is made of the number of parameters for a given value of λ. Figure 5 below relates the error in the prediction of the attenuation value to the number of perceptrons in the network.

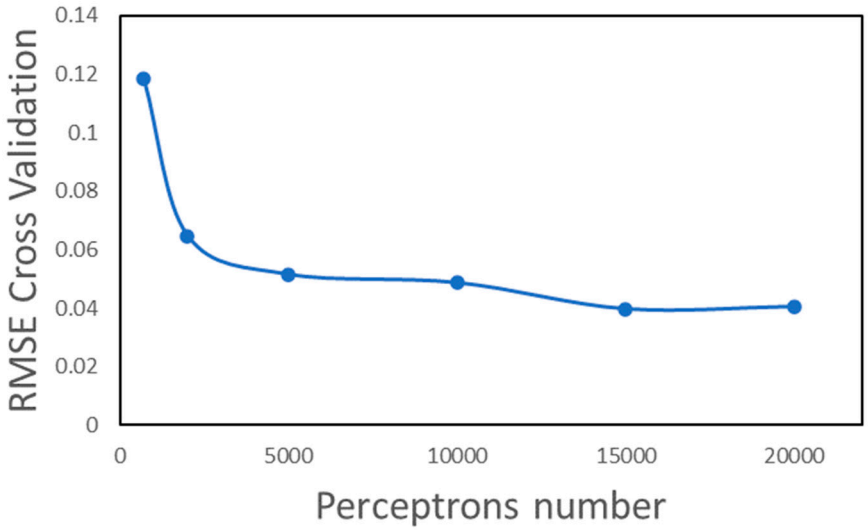

Figure 5. RMSE cross-validation values for setting the number of perceptrons. It is set up to 15,575 distributed in 7 layers.

The optimal number of perceptrons of the neural network is 15,575. Following this architecture, the value of λ is optimized by choosing values of 0.1, 0.01, 0.001, and 0.0001, resulting in the following (Figure 6).

The result suggests the best value of λ. The root mean sum square error (RMSE) remains constant when λ is near to 0.001. Then, the optimal value is set up to 0.001. The value of λ is used in the backpropagation algorithm to avoid bias and overfitting [118,119]. Figure 7 shows the loss function versus the number of epoch. It is necessary for 10,000 epoch to obtain a loss cost value equal a 0.0332.

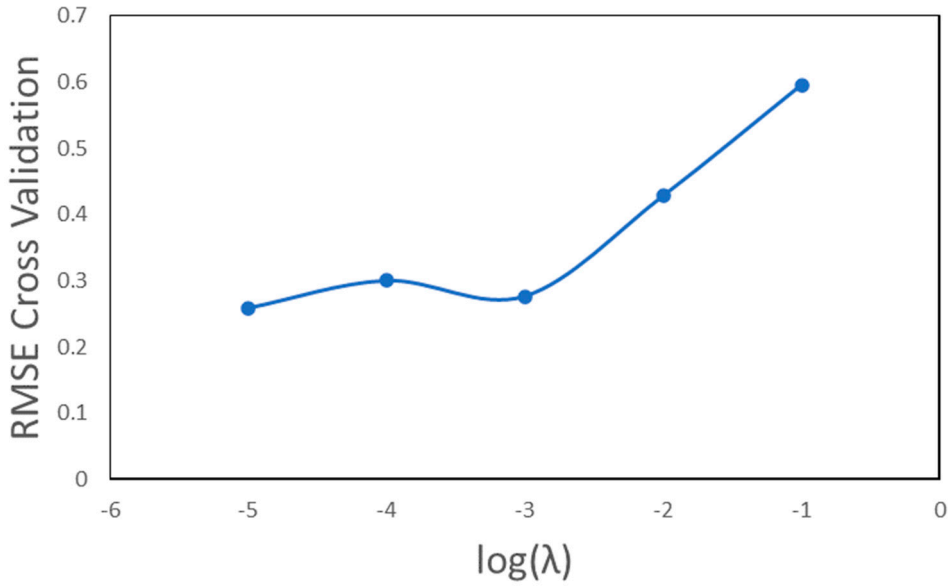

Figure 6. RMSE cross-validation. The optimal value of λ is set near to 10^{-3}.

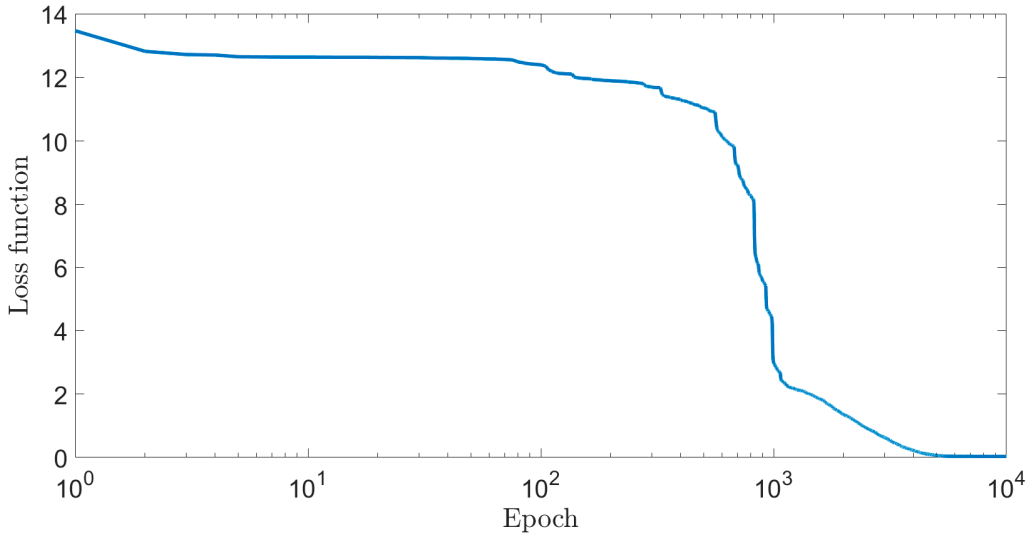

Figure 7. Loss function versus the number of epoch. The optimal value of epoch is 10,000 giving a loss cost value 0.0332.

5. Results

Figure 8 shows the solution obtained for the proposed deep learning model. This is the 3D view of the neural network, as can be seen in Figure 3 (Figure 8a), where the values taken in the greenhouse appear as blue dots. The x-axis and y-axis are distance (d) and height (h), respectively, in meters. The z-axis is values when evaluating the deep neural network $L_{foliage}\ (d, h)$ for the distance and height data. Figure 8b shows the residual values between measured data and those calculated with the deep neural network.

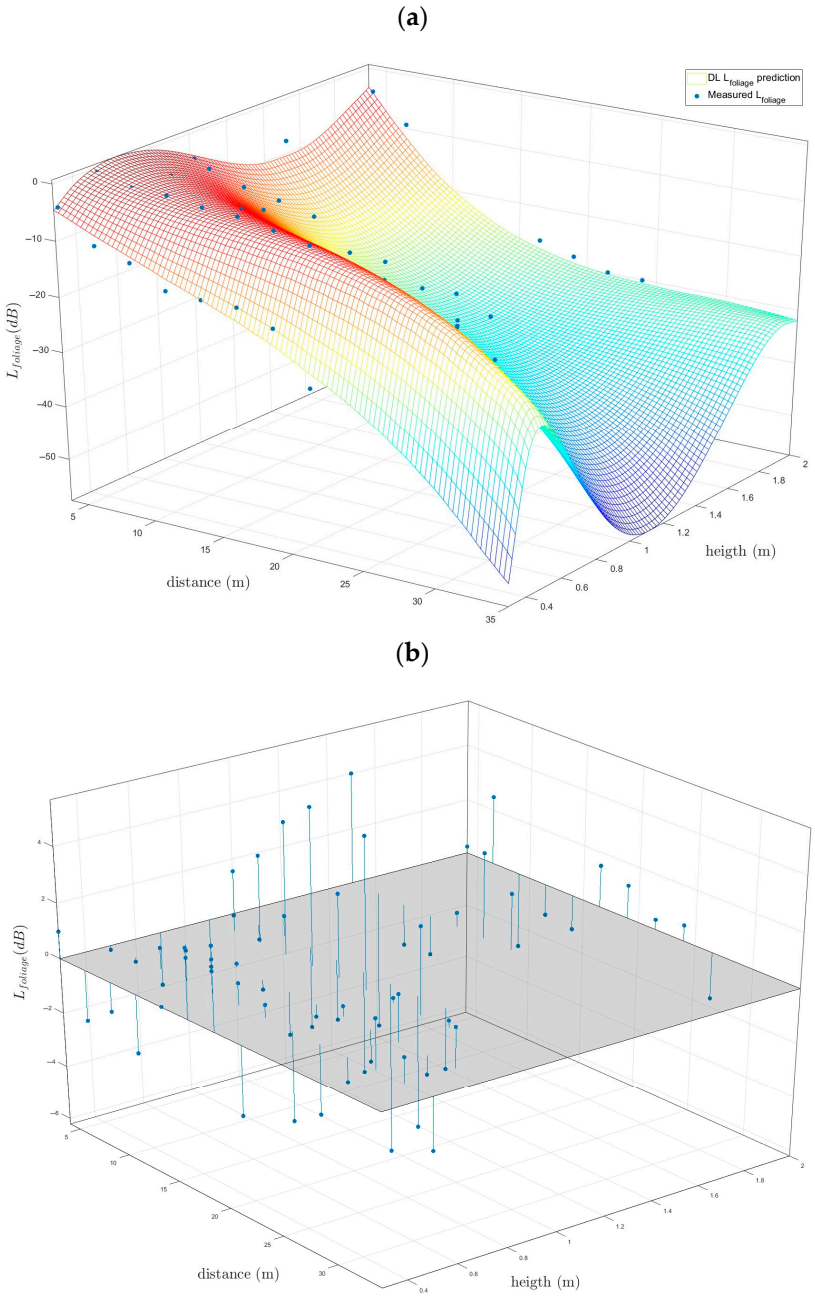

Figure 8. (**a**) The black dots represent the values taken in field tests, together with the $L_{foliage}\ (d, h)$ optimized for the deep learning model. (**b**) Difference between measured and predicted data are the Residual values of $L_{foliage}\ (d, h)$.

The cross-validation of parameters reveals the quality of the new model. R^2 and Q^2, these values were 0.966 and 0.957. The RMSECV was 1.98. The deep neural network was also validated by permutation testing.

The values for the evaluation of the multi-parametric optimised function are presented in Table 1. The 0.966 value was the adjusted R^2.

Table 1. Statistical Quality Assessment of the proposed deep learning model.

	R^2	R^2_{Adj}	MSE	RMSE	MAPE	AIC	SBC
$L_{foliage}(d, h)$	0.966	0.964	3.39	1.98	0.113	432	221

The radio wave attenuation of deep learning for vegetation in a tomato greenhouse developed in this research improved the predictions of other models; the R^2 was 0.966. Likewise, the adjusted R^2 in the two scenarios was very close, at around 0.964. The MSE and RMSE values were near, which means the deep learning model has a good fit. The AIC and SBC are of similar magnitude, which suggests that no information was lost when applying either model.

The deep learning model was compared with other measurements taken in field tests. These measurements were made in 2020 and 2018, all of them were greenhouses producing the same type of tomato (tinkwino), at the peak of production and leafiness (February). The values summarized in Table 2 for all greenhouses, and it reveals that the deep learning model obtained worked well.

Table 2. Statistical quality assessment of the proposed deep learning model for other five greenhouses measurements.

	Location	Year	R^2	R^2_{Adj}	MSE	RMSE	MAPE	AIC	SBC
$L_{foliage}(d,h)$	Cañada	2020	0.935	0.933	8.32	2.88	0.398	462	250
$L_{foliage}(d,h)$	Retamar	2020	0.926	0.913	8.75	2.95	0.257	465	254
$L_{foliage}(d,h)$	Alquián	2020	0.913	0.900	9.52	3.08	0.238	475	260
$L_{foliage}(d,h)$	Níjar	2020	0.908	0.910	11.15	3.33	0.594	485	271
$L_{foliage}(d,h)$	Cañada	2018	0.915	0.903	10.17	3.19	0.595	476	264

The generalized error of the model was evaluated with real values for its fit. Table 2 reveals that the R^2 parameter was between 0.908 and 0.935. The generalized R^2 can be considered as its mean. The mean of R^2 was 0.920. RMSE was between 2.88 and 3.33. The generalized RMSE can be considered as its mean was 3.08. This error was larger than that obtained with the model fit values, which is to be expected

6. Discussion

These results demonstrate the applicability of the novel approach. In addition, field tests established that the highest coverage between the R_x and T_x nodes occurred when the height of the nodes' antennas was 0.5 m from the ground. Using the deep learning model proposed, the behavioral model of the attenuation of radio waves passing through vegetation was in the 2.4 GHz band widely used by the IEEE 802.15.4 standard. The evaluation of the statistical quality of the models between deep learning and regularised regression with 20 parameters is shown in Table 3, with the former giving better values.

Table 3. Statistical quality assessment comparison between deep learning model and regularized regressions.

	Model	R^2	R^2_{Adj}	MSE	RMSE	MAPE	AIC	SBC
$L_{foliage}(d,h)$	Deep Learning	0.966	0.964	3.39	1.98	0.113	432	221
$L_{foliage}(d,h)$	Regularized Regressions	0.948	0.946	5.27	2.29	0.167	410	199

As this research has proven, the main problem with predicting attenuation lies in its highly non-linear analytical function. To obtain an expression adjusted to this non-linearity, a 5-degree polynomial with all possible combinations for two variables was needed to be added to the analytical expression usually used. With a non-linear adjustment and performing a novel dimensionality reduction on a regularized cost function, the generalized accuracy of this model is 0.906.

For a high degree of accuracy, the only technique which can handle highly non-linear analytical functions is deep learning. This technique has evolved with the evolution of computation and is currently used for a multitude of systems precisely because of its potential to increase the accuracy of the predictions it makes.

The important feature of this manuscript lies in the fact that it is the first application of the deep learning model for the prediction of electromagnetic attenuations inside a tomato greenhouse; for this case, there is no model in the literature, and it also lays the foundation for further experiments with various crops that, on this architecture, the deep learning model will be able to make attenuation predictions on any greenhouse with any crop. This deep learning model has achieved such an impressive performance that it improves the generalized accuracy by 2 points and reduces the mean square error by one-third.

7. Conclusions

Experimental measurements of radio wave attenuation inside a tomato greenhouse have been carried out using a wireless sensor network using the 2400 MHz frequency band. Previously recorded attenuation values compared to other empirical attenuation models showed significant errors. It is useful for the planning of the distribution and the deployment of WSN nodes in WSNs applied to precision agriculture.

To enhance the predictions of these empirical models, deep learning neural networks of our own were developed. We ensure that there is no over-fitting or bias in the prediction of the neural network parameters since a L-Curve method is applied. The deep learning model, based on the EDM has the simplicity of using only the variables of antenna height and node distance compared to other models, with height affecting the results the most. The evaluation of the deep learning model demonstrates reliability, obtaining 0.966 for R^2 and 0.964 for $R^2_{adj,}$ while the generalized error was 0.920 for R^2 and 0.912 for R^2_{adj}. The methodology presented will serve to generate a deep learning model of the attenuation behavior of wireless signals when passing through vegetation. The model is composed of the exponential attenuation and the compensation function associated with the environment where the radio wave is transmitted. In summary, deep learning models are able to learn from a small amount of labeled data and make use of large amounts of unlabeled data, which can be especially useful in cases where it is difficult or expensive to obtain a large amount of labeled data. In general, deep learning models have a number of advantages that make them well-suited for tasks involving complex, high-dimensional data, as has been the proven case for signal attenuation within a tomato-growing greenhouse. We understand that this is one more step towards the modernization of agriculture, as automation will involve wireless communication inside the greenhouse. Future research will focus on evaluating or refining the model taking into consideration crop growth.

Author Contributions: Conceptualization, M.D., J.A.H.-T., D.C.-P. and A.C.-P.; data curation, D.C.-P., J.A.H.-T. and F.M.A.-C.; formal analysis, D.C.-P., M.D., J.A.H.-T., F.M.A.-C., J.A.M.-L. and A.C.-P.; funding acquisition, D.C.-P., F.M.-A. and A.C.-P.; investigation, D.C.-P., M.D., J.A.H.-T., F.M.A.-C., J.A.M.-L. and A.C.-P.; methodology, D.C.-P., M.D., J.A.H.-T., F.M.A.-C., J.A.M.-L. and A.C.-P.; project administration, D.C.-P., M.D., F.M.-A. and F.M.A.-C.; resources, D.C.-P.; software, D.C.-P., F.M.A.-C. and A.C.-P.; supervision, M.D. and J.A.H.-T.; validation, M.D., J.A.H.-T., F.M.A.-C., J.A.M.-L., F.M.-A. and A.C.-P.; writing—original draft, D.C.-P., F.M.A.-C. and A.C.-P.; writing—review & editing, J.A.H.-T. and F.M.-A. All authors have read and agreed to the published version of the manuscript.

Funding: This research received support from the AUIP (Iberoamerican University Association for Postgraduate Studies), by the Spanish Ministry of Science, Innovation, and Universities under the programme "Proyectos de I+D de Generacion de Conocimiento" of the national programme for the generation of scientific and technological knowledge and strengthening of the R+D+I system through grant number PGC2018-098813-B-C33 and by UAL-FEDER 2020, Ref. UAL2020-TIC-A2080.

Data Availability Statement: The data can be found at: available online: https://data.mendeley.com/datasets/nhk3gs7gmm/1 (accessed on 28 July 2022).

Conflicts of Interest: The authors declare no conflict of interest.

References

1. Bartkowiak, A.M. Energy-saving and low-emission livestock buildings in the concept of a smart farming. *J. Water Land Dev.* **2021**, *51*, 272–278. [CrossRef]
2. Sagheer, A.; Mohammed, M.; Riad, K.; Alhajhoj, M. A Cloud-Based IoT Platform for Precision Control of Soilless Greenhouse Cultivation. *Sensors* **2021**, *21*, 223. [CrossRef] [PubMed]
3. Akhigbe, B.; Munir, K.; Akinade, O.; Akanbi, L.; Oyedele, L. IoT Technologies for Livestock Management: A Review of Present Status, Opportunities, and Future Trends. *Big Data Cogn. Comput.* **2021**, *5*, 10. [CrossRef]
4. Mahbub, M. A smart farming concept based on smart embedded electronics, internet of things and wireless sensor network. *Internet Things* **2020**, *9*, 100161. [CrossRef]
5. Andrianto, H.; Suhardi; Faizal, A. Development of smart greenhouse system for hydroponic agriculture. In Proceedings of the 2020 International Conference on Information Technology Systems and Innovation, Padang, Indonesia, 19–23 October 2020; pp. 335–340. [CrossRef]
6. Latino, M.E.; Menegoli, M.; Corallo, A. Agriculture Digitalization: A Global Examination Based on Bibliometric Analysis. *IEEE Trans. Eng. Manag.* **2022**, 1–16. [CrossRef]
7. Ullah, M.; Narayanan, A.; Wolff, A.; Nardelli, P.H.J. Unified Framework to Select an IoT Platform for Industrial Energy Management Systems. In Proceedings of the 2021 44th International Convention on Information, Communication and Electronic Technology, Opatija, Croatia, 27 September–1 October 2021; pp. 950–955. [CrossRef]
8. Dastjerdi, A.V.; Buyya, R. Fog Computing: Helping the Internet of Things Realize Its Potential. *Computer* **2016**, *49*, 112–116. [CrossRef]
9. Pflanzner, T.; Hovari, M.; Vass, I.; Kertesz, A. Designing an IoT-Cloud Gateway for the Internet of Living Things. *Commun. Comput. Inf. Sci.* **2020**, *1218*, 23–41. [CrossRef]
10. Sorri, K.; Mustafee, N.; Seppänen, M. Revisiting IoT definitions: A framework towards comprehensive use. *Technol. Forecast. Soc. Chang.* **2022**, *179*, 121623. [CrossRef]
11. Vanitha, V.; Raj, C.S.; Kumar, K.M.; Sebastian, J. Design and Development of an Effective Smart Garbage System using the Internet of Things. *J. Physics Conf. Ser.* **2021**, *2040*, 012033. [CrossRef]
12. Arrubla-Hoyos, W.; Ojeda-Beltrán, A.; Solano-Barliza, A.; Rambauth-Ibarra, G.; Barrios-Ulloa, A.; Cama-Pinto, D.; Arrabal-Campos, F.M.; Martínez-Lao, J.A.; Cama-Pinto, A.; Manzano-Agugliaro, F. Precision Agriculture and Sensor Systems Applications in Colombia through 5G Networks. *Sensors* **2022**, *22*, 7295. [CrossRef]
13. Barrios-Ulloa, A.; Ariza-Colpas, P.P.; Sánchez-Moreno, H.; Quintero-Linero, A.P.; De la Hoz-Franco, E. Modeling Radio Wave Propagation for Wireless Sensor Networks in Vegetated Environments: A Systematic Literature Review. *Sensors* **2022**, *22*, 5285. [CrossRef] [PubMed]
14. Sishodia, R.P.; Ray, R.L.; Singh, S.K. Applications of Remote Sensing in Precision Agriculture: A Review. *Remote. Sens.* **2020**, *12*, 3136. [CrossRef]
15. Suresh, P.; Daniel, J.V.; Parthasarathy, V.; Aswathy, R.H. A state of the art review on the Internet of Things (IoT) history, technology and fields of deployment. In Proceedings of the 2014 International Conference on Science Engineering and Management Research, Chennai, India, 27–29 November 2014. [CrossRef]
16. Mahajan, H.B.; Badarla, A. Cross-Layer Protocol for WSN-Assisted IoT Smart Farming Applications Using Nature Inspired Algorithm. *Wirel. Pers. Commun.* **2021**, *121*, 3125–3149. [CrossRef]
17. Raheemah, A.; Sabri, N.; Salim, M.S.; Ehkan, P.; Kamaruddin, R.; Ahmad, R.B.; Jaafar, M.N.; Aljunid, S.A.; Chemat, M.H. Influences of parts of tree on propagation path losses for wsn deployment in greenhouse environments. *J. Theor. Appl. Inf. Technol.* **2015**, *81*, 552–557.
18. Li, P.; Peng, Y.; Wang, J. Propagation characteristics of 2.4 GHz radio wave in greenhouse of green peppers. Nongye Jixie Xuebao/Trans. *Chin. Soc. Agric. Mach.* **2014**, *45*, 251–255. [CrossRef]
19. Raheemah, A.; Sabri, N.; Salim, M.; Ehkan, P.; Ahmad, R.B. New empirical path loss model for wireless sensor networks in mango greenhouses. *Comput. Electron. Agric.* **2016**, *127*, 553–560. [CrossRef]
20. Vougioukas, S.; Anastassiu, H.; Regen, C.; Zude, M. Influence of foliage on radio path losses (PLs) for wireless sensor network (WSN) planning in orchards. *Biosyst. Eng.* **2013**, *114*, 454–465. [CrossRef]
21. Cama-Pinto, D.; Damas, M.; Holgado-Terriza, J.A.; Gómez-Mula, F.; Cama-Pinto, A. Path Loss Determination Using Linear and Cubic Regression Inside a Classic Tomato Greenhouse. *Int. J. Environ. Res. Public Health* **2019**, *16*, 1744. [CrossRef]
22. Cama-Pinto, D.; Damas, M.; Holgado-Terriza, J.A.; Arrabal-Campos, F.M.; Gómez-Mula, F.; Martínez-Lao, J.A.M.; Cama-Pinto, A. Empirical Model of Radio Wave Propagation in the Presence of Vegetation inside Greenhouses Using Regularized Regressions. *Sensors* **2020**, *20*, 6621. [CrossRef]
23. França, R.P.; Monteiro, A.C.B.; Arthur, R.; Iano, Y. An Overview of Internet of Things Technology Applied on Precision Agriculture Concept. *Precis. Agric. Technol. Food Secur. Sustain.* **2020**, 47–70. [CrossRef]
24. Boursianis, A.D.; Papadopoulou, M.S.; Diamantoulakis, P.; Liopa-Tsakalidi, A.; Barouchas, P.; Salahas, G.; Karagiannidis, G.; Wan, S.; Goudos, S.K. Internet of Things (IoT) and Agricultural Unmanned Aerial Vehicles (UAVs) in smart farming: A comprehensive review. *Internet Things* **2022**, *18*, 100187. [CrossRef]

25. Sott, M.K.; Nascimento, L.D.S.; Foguesatto, C.R.; Furstenau, L.B.; Faccin, K.; Zawislak, P.A.; Mellado, B.; Kong, J.D.; Bragazzi, N.L. A Bibliometric Network Analysis of Recent Publications on Digital Agriculture to Depict Strategic Themes and Evolution Structure. *Sensors* **2021**, *21*, 7889. [CrossRef] [PubMed]
26. Khandelwal, D.D.; Singhal, M. Developing a low-cost weather monitoring system for data-sparse regions of the Himalayas. *Weather* **2021**, *76*, 60–64. [CrossRef]
27. Montoya, F.G.; Gomez, J.; Manzano-Agugliaro, F.; Cama, A.; García-Cruz, A.; De La Cruz, J.L. 6LoWSoft: A software suite for the design of outdoor environmental measurements. *J. Food Agric. Environ.* **2013**, *11*, 2584–2586.
28. Salim, C.; Mitton, N. K-predictions based data reduction approach in WSN for smart agriculture. *Computing* **2021**, *103*, 509–532. [CrossRef]
29. Wu, H.; Miao, Y.; Li, F.; Zhu, L. Empirical Modeling and Evaluation of Multi-Path Radio Channels on Wheat Farmland Based on Communication Quality. *Trans. ASABE* **2016**, *59*, 759–767. [CrossRef]
30. Maiolo, L.; Polese, D. Advances in sensing technologies for smart monitoring in precise agriculture. In Proceedings of the 10th International Conference on Sensor Networks, Online, 9–10 February 2021; pp. 151–158.
31. Sathish, C.; Srinivasan, K. An artificial bee colony algorithm for efficient optimized data aggregation to agricultural IoT devices application. *J. Appl. Sci. Eng.* **2021**, *24*, 927–936. [CrossRef]
32. Hsiao, S.-J.; Sung, W.-T. A Study on Using a Wireless Sensor Network to Design a Plant Monitoring System. *Intell. Autom. Soft Comput.* **2021**, *27*, 359–377. [CrossRef]
33. Xuanrong, P.; Tingdong, Y.; Yuesheng, W. Research and design of precision irrigation system based on artificial neural network. In Proceedings of the 2018 Chinese Control and Decision Conference (CCDC), Shenyang, China, 9–11 June 2018; pp. 3865–3870.
34. Wang, J.; Peng, Y.; Li, P. Propagation Characteristics of Radio Wave in Plastic Greenhouse. In *IFIP Advances in Information and Communication Technology*; Springer: Cham, Switzerland, 2016; pp. 208–215. [CrossRef]
35. Huang, C.-N.; Chan, C.-T. A ZigBee-Based Location-Aware Fall Detection System for Improving Elderly Telecare. *Int. J. Environ. Res. Public Health* **2014**, *11*, 4233. [CrossRef]
36. Rao, Y.; Jiang, Z.-H.; Lazarovitch, N. Investigating signal propagation and strength distribution characteristics of wireless sensor networks in date palm orchards. *Comput. Electron. Agric.* **2016**, *124*, 107–120. [CrossRef]
37. Shaw, J.A. Radiometry and the Friis transmission equation. *Am. J. Phys.* **2012**, *81*, 33–37. [CrossRef]
38. Friis, H. A Note on a Simple Transmission Formula. *Proc. IRE* **1946**, *34*, 254–256. [CrossRef]
39. Biggelaar, A.J.V.D.; Geluk, S.J.; Jamroz, B.F.; Williams, D.F.; Smolders, A.B.; Johannsen, U.; Bronckers, L.A. Accurate Gain Measurement Technique for Limited Antenna Separations. *IEEE Trans. Antennas Propag.* **2021**, *69*, 6772–6782. [CrossRef]
40. Kim, Y.; Boo, S.; Kim, G.; Kim, N.; Lee, B. Wireless Power Transfer Efficiency Formula Applicable in Near and Far Fields. *J. Electromagn. Eng. Sci.* **2019**, *19*, 239–244. [CrossRef]
41. Bensky, A. (Ed.) *Chapter 2—Radio Propagation, Short-range Wireless Communication*, 3rd ed.; Newnes: Oxford, UK, 2019; pp. 11–41. ISBN 9780128154052. [CrossRef]
42. Bowrothu, R.; Yoon, Y.K. Low Loss Cu/Co Metaconductor Based Array Antenna in KaBand for 5G Applications. In Proceedings of the 2020 IEEE International Symposium on Antennas and Propagation and North American Radio Science Meeting, Toronto, ON, Canada, 5–10 July 2020; pp. 35–36. [CrossRef]
43. Mahesh, G.; Balachander, D.; Rao, T.R. RF Propagation Measurements in Agricultural Fields for Wireless Sensor Communications. In Proceedings of the IEEE International Conference on Circuit, Power and Computing Technologies (ICCPCT), Nagercoil, India, 20–21 March 2013; pp. 808–812. [CrossRef]
44. Rao, T.R.; Balachander, D.; Tiwari, N. UHF short-range pathloss measurements in forest & plantation environments for wireless sensor networks. In Proceedings of the IEEE International Conference on Communication Systems (ICCS), Singapore, 21–23 November 2012; pp. 194–198. [CrossRef]
45. Frenzel, L. Millimeter Waves Will Expand the Wireless Future (2013). Electronic Design (6). Available online: https://www.electronicdesign.com/home/whitepaper/21802894/millimeter-waves-will-expand-the-wireless-future-pdf-download (accessed on 30 October 2022).
46. Agrawal, S.K.; Garg, P. Calculation of channel capacity and rician factor in the presence of vegetation in higher altitude platforms communication systems. In Proceedings of the 15th International Conference on Advanced Computing and Communications (ADCOM), Guwahati, India, 18–21 December 2007; pp. 243–248.
47. Sabri, N.; Mohammed, S.S.; Fouad, S.; Syed, A.A.; Al-Dhief, F.T.; Raheemah, A. Investigation of Empirical Wave Propagation Models in Precision Agriculture. *MATEC Web Conf.* **2018**, *150*, 06020. [CrossRef]
48. Lytaev, M.S.; Vladyko, A.G. Split-step Padé Approximations of the Helmholtz Equation for Radio Coverage Prediction over Irregular Terrain. In Proceedings of the 2018 Advances in Wireless and Optical Communications (RTUWO), Riga, Latvia, 15–16 November 2018; pp. 179–184.
49. Liu, H.-X.; Yan, H.-L.; Jia, N.; Tang, S.; Cong, D.; Yang, B.; Li, Z.; Zhang, Y.; Esling, C.; Zhao, X.; et al. Machine-learning-assisted discovery of empirical rule for inherent brittleness of full Heusler alloys. *J. Mater. Sci. Technol.* **2022**, *131*, 1–13. [CrossRef]
50. Figueroa, J.D.O.; Reeves, J.S.; McPherron, S.P.; Tennie, C. A proof of concept for machine learning-based virtual knapping using neural networks. *Sci. Rep.* **2021**, *11*, 19966. [CrossRef]

51. Wang, F.; Zhang, Z.; Wang, G.; Wang, Z.; Li, M.; Liang, W.; Gao, J.; Wang, W.; Chen, D.; Feng, Y.; et al. Machine learning and theoretical analysis release the non-linear relationship among ozone, secondary organic aerosol and volatile organic compounds. *J. Environ. Sci.* **2022**, *114*, 75–84. [CrossRef]
52. Matsuo, Y.; LeCun, Y.; Sahani, M.; Precup, D.; Silver, D.; Sugiyama, M.; Uchibe, E.; Morimoto, J. Deep learning, reinforcement learning, and world models. *Neural Netw.* **2022**, *152*, 267–275. [CrossRef]
53. Sharma, S.; Mandal, P.K. A Comprehensive Report on Machine Learning-based Early Detection of Alzheimer's Disease using Multi-modal Neuroimaging Data. *ACM Comput. Surv.* **2023**, *55*, 3492865. [CrossRef]
54. Srinivasan, P.; Jagatheeswari, P. Machine Learning Controller for DFIG Based Wind Conversion System. *Intell. Autom. Soft Comput.* **2023**, *35*, 381–397. [CrossRef]
55. Agliari, E.; Alemanno, F.; Barra, A.; De Marzo, G. The emergence of a concept in shallow neural networks. *Neural Netw.* **2022**, *148*, 232–253. [CrossRef] [PubMed]
56. Mishra, C.; Gupta, D.L. Deep Machine Learning and Neural Networks: An Overview. *IAES Int. J. Artif. Intell. (IJ-AI)* **2017**, *6*, 66–73. [CrossRef]
57. Muthukumaran, S.; Geetha, P.; Ramaraj, E. Multi-Objective Optimization with Artificial Neural Network Based Robust Paddy Yield Prediction Model. *Intell. Autom. Soft Comput.* **2023**, *35*, 215–230. [CrossRef]
58. Li, X.; He, J.; Huang, Y.; Li, J.; Liu, X.; Dai, J. Predicting the factors influencing construction enterprises' adoption of green development behaviors using artificial neural network. *Humanit. Soc. Sci. Commun.* **2022**, *9*, 1–12. [CrossRef]
59. Mrabti, N.N.; Mrabti, H.N.; Khalil, Z.; Bouyahya, A.; Mohammed, E.-R.; Dguigui, K.; Doudach, L.; Zengin, G.; Elhallaoui, M. Molecular Docking and QSAR Studies for Modeling the Inhibitory Activity of Pyrazole-benzimidazolone Hybrids as Novel Inhibitors of Human 4-hydroxyphenylpyruvate dioxygenase Against Type I Tyrosinemia Disease. *Biointerface Res. Appl. Chem.* **2022**, *13*, 38. [CrossRef]
60. Dai, D. An Introduction of CNN: Models and Training on Neural Network Models. In Proceedings of the 2021 International Conference on Big Data, Artificial Intelligence and Risk Management, Shanghai, China, 5–7 November 2021; pp. 135–138. [CrossRef]
61. Wickramanayake, S.; Hsu, W.; Lee, M.L. Comprehensible Convolutional Neural Networks via Guided Concept Learning. In Proceedings of the International Joint Conference on Neural Networks, Shenzhen, China, 18–22 July 2021. [CrossRef]
62. Vaz, J.M.; Balaji, S. Convolutional neural networks (CNNs): Concepts and applications in pharmacogenomics. *Mol. Divers.* **2021**, *25*, 1569–1584. [CrossRef]
63. Sergeev, D. *Classification of human actions using task fMRI images (2019) CEUR Workshop Proceedings*; CEUR Workshop Proceedings: Tenerife, Spain, 2019; Volume 2523, pp. 395–403.
64. Berhich, A.; Belouadha, F.-Z.; Kabbaj, M.I. A location-dependent earthquake prediction using recurrent neural network algorithms. *Soil Dyn. Earthq. Eng.* **2022**, *161*, 107389. [CrossRef]
65. Escamilla-Rivera, C.; Carvajal, M.; Zamora, C.; Hendry, M. Neural networks and standard cosmography with newly calibrated high redshift GRB observations. *J. Cosmol. Astropart. Phys.* **2022**, *2022*, 52. [CrossRef]
66. Farris, A.B.; Vizcarra, J.; Amgad, M.; Cooper, L.A.D.; Gutman, D.; Hogan, J. Artificial intelligence and algorithmic computational pathology: An introduction with renal allograft examples. *Histopathology* **2021**, *78*, 791–804. [CrossRef]
67. Kavlakoglu, E. AI vs. Machine Learning vs. Deep Learning vs. Neural Networks: What's the Difference? IBM Blog. 2020. Available online: https://www.ibm.com/cloud/blog/ai-vs-machine-learning-vs-deep-learning-vs-neural-networks (accessed on 28 July 2022).
68. Bengio, Y.; Lecun, Y.; Hinton, G. Deep learning for AI. *Commun. ACM* **2021**, *64*, 58–65. [CrossRef]
69. Franchini, G.; Ruggiero, V.; Porta, F.; Zanni, L. Neural architecture search via standard machine learning methodologies. *Math. Eng.* **2023**, *5*, 1–21. [CrossRef]
70. LeCun, Y. 1.1 Deep Learning Hardware: Past. Present, and Future Digest of Technical Papers. In Proceedings of the IEEE International Solid-State Circuits Conference, San Francisco, CA, USA, 17–21 February 2019; pp. 12–19. [CrossRef]
71. Ranzato, M.; Hinton, G.; LeCun, Y. Guest Editorial: Deep Learning. *Int. J. Comput. Vis.* **2015**, *113*, 1–2. [CrossRef]
72. Ito, S.; Hayashi, T. Radio Propagation Estimation in a Long-Range Environment using a Deep Neural Network. In Proceedings of the 15th European Conference on Antennas and Propagation, Düsseldorf, Germany, 22–26 March 2021. [CrossRef]
73. Moraitis, N.; Tsipi, L.; Vouyioukas, D.; Gkioni, A.; Louvros, S. On the Assessment of Ensemble Models for Propagation Loss Forecasts in Rural Environments. *IEEE Wirel. Commun. Lett.* **2022**, *11*, 1097–1101. [CrossRef]
74. Bogdándy, B.; Tóth, Z. Inversion of artificial neural networks for WiFi RSSI propagation modeling. *CEUR Workshop Proc.* **2021**, *2874*, 67–76.
75. Seretis, A.; Zhang, X.; Zeng, K.; Sarris, C.D. Artificial neural network models for radiowave propagation in tunnels. *IET Microw. Antennas Propag.* **2020**, *14*, 1198–1208. [CrossRef]
76. Castillo-Díaz, F.J.; Marín-Guirao, J.I.; Belmonte-Ureña, L.J.; Tello-Marquina, J.C. Effect of Repeated Plant Debris Reutilization as Organic Amendment on Greenhouse Soil Fertility. *Int. J. Environ. Res. Public Health* **2021**, *18*, 11544. [CrossRef] [PubMed]
77. Caparrós-Martínez, J.L.; Rueda-Lópe, N.; Milán-García, J.; Valenciano, J.D.P. Public policies for sustainability and water security: The case of Almeria (Spain). *Glob. Ecol. Conserv.* **2020**, *23*, e01037. [CrossRef]
78. Massa, D.; Magán, J.J.; Montesano, F.F.; Tzortzakis, N. Minimizing water and nutrient losses from soilless cropping in southern Europe. *Agric. Water Manag.* **2020**, *241*, 106395. [CrossRef]

79. Pinna-Hernández, M.; Fernández, F.; Segura, J.; López, J. Solar Drying of Greenhouse Crop Residues for Energy Valorization: Modeling and Determination of Optimal Conditions. *Agronomy* **2020**, *10*, 2001. [CrossRef]
80. Camacho-Arévalo, R.; García-Delgado, C.; Mayans, B.; Antón-Herrero, R.; Cuevas, J.; Segura, M.; Eymar, E. Sulfonamides in Tomato from Commercial Greenhouses Irrigated with Reclaimed Wastewater: Uptake, Translocation and Food Safety. *Agronomy* **2021**, *11*, 1016. [CrossRef]
81. Martin-Gorriz, B.; Maestre-Valero, J.; Gallego-Elvira, B.; Marín-Membrive, P.; Terrero, P.; Martínez-Alvarez, V. Recycling drainage effluents using reverse osmosis powered by photovoltaic solar energy in hydroponic tomato production: Environmental footprint analysis. *J. Environ. Manag.* **2021**, *297*, 113326. [CrossRef] [PubMed]
82. Aznar-Sánchez, J.A.; Velasco-Muñoz, J.F.; García-Arca, D.; López-Felices, B. Identification of Opportunities for Applying the Circular Economy to Intensive Agriculture in Almería (South-East Spain). *Agronomy* **2020**, *10*, 1499. [CrossRef]
83. Duque-Acevedo, M.; Belmonte-Ureña, L.J.; Toresano-Sánchez, F.; Camacho-Ferre, F. Biodegradable Raffia as a Sustainable and Cost-Effective Alternative to Improve the Management of Agricultural Waste Biomass. *Agronomy* **2020**, *10*, 1261. [CrossRef]
84. Manríquez-Altamirano, A.; Sierra-Pérez, J.; Muñoz, P.; Gabarrell, X. Analysis of urban agriculture solid waste in the frame of circular economy: Case study of tomato crop in integrated rooftop greenhouse. *Sci. Total Environ.* **2020**, *734*, 139375. [CrossRef]
85. Téllez, M.; Cabello, T.; Gámez, M.; Burguillo, F.; Rodríguez, E. Comparative study of two predatory mites *Amblyseius swirskii* Athias-Henriot and Transeius montdorensis (Schicha) by predator-prey models for improving biological control of greenhouse cucumber. *Ecol. Model.* **2020**, *431*, 109197. [CrossRef]
86. Honoré, M.N.; Belmonte-Ureña, L.J.; Navarro-Velasco, A.; Camacho-Ferre, F. Profit Analysis of Papaya Crops under Greenhouses as an Alternative to Traditional Intensive Horticulture in Southeast Spain. *Int. J. Environ. Res. Public Health* **2019**, *16*, 2908. [CrossRef]
87. Martínez-Valderrama, J.; Guirado, E.; Maestre, F.T. Discarded food and resource depletion. *Nat. Food* **2020**, *1*, 660–662. [CrossRef]
88. Cama-Pinto, D.; Holgado-Terriza, J.A.; Damas-Hermoso, M.; Gómez-Mula, F.; Cama-Pinto, A. Radio Wave Attenuation Measurement System Based on RSSI for Precision Agriculture: Application to Tomato Greenhouses. *Inventions* **2021**, *6*, 66. [CrossRef]
89. Şen, Z.; Şişman, E.; Kızılöz, B. A new innovative method for model efficiency performance. *Water Supply* **2022**, *22*, 589–601. [CrossRef]
90. Lyu, Z.; Yu, Y.; Samali, B.; Rashidi, M.; Mohammadi, M.; Nguyen, T.N.; Nguyen, A. Back-Propagation Neural Network Optimized by K-Fold Cross-Validation for Prediction of Torsional Strength of Reinforced Concrete Beam. *Materials* **2022**, *15*, 1477. [CrossRef]
91. Song, X.; Li, K.; Dai, K.; Wang, X.; Du, H.; Zhao, H. A random-forest-assisted artificial-neural-network method for analysis of steel using laser-induced breakdown spectroscopy. *Optik* **2022**, *249*, 168214. [CrossRef]
92. Short, S.M.; Cogdill, R.P.; Anderson, C.A. Determination of figures of merit for near-infrared and raman spectrometry by net analyte signal analysis for a 4-component solid dosage system. *AAPS PharmSciTech* **2007**, *8*, 109–119. [CrossRef]
93. Peng, Y.; Knadel, M.; Gislum, R.; Schelde, K.; Thomsen, A.; Greve, M.H. Quantification of SOC and Clay Content Using Visible Near-Infrared Reflectance–Mid-Infrared Reflectance Spectroscopy with Jack-Knifing Partial Least Squares Regression. *Soil Sci.* **2014**, *179*, 325–332. [CrossRef]
94. Yoon, S.; Choi, J.; Moon, S.-J.; Choi, J. Determination and Quantification of Heavy Metals in Sediments through Laser-Induced Breakdown Spectroscopy and Partial Least Squares Regression. *Appl. Sci.* **2021**, *11*, 7154. [CrossRef]
95. Yap, X.Y.; Chia, K.S.; Tee, K.S. A Portable Gas Pressure Control and Data Acquisition System using Regression Models. *Int. J. Electr. Eng. Inform.* **2021**, *13*, 242–251. [CrossRef]
96. Obisesan, K.A.; Neri, S.; Bugnicourt, E.; Campos, I.; Rodriguez-Turienzo, L. Determination and Quantification of the Distribution of CN-NL Nanoparticles Encapsulating Glycyrrhetic Acid on Novel Textile Surfaces with Hyperspectral Imaging. *J. Funct. Biomater.* **2020**, *11*, 32. [CrossRef]
97. Chang, W.; Ji, X.; Wang, L.; Liu, H.; Zhang, Y.; Chen, B.; Zhou, S. A Machine-Learning Method of Predicting Vital Capacity Plateau Value for Ventilatory Pump Failure Based on Data Mining. *Healthcare* **2021**, *9*, 1306. [CrossRef] [PubMed]
98. Faroughi, S.A.; Roriz, A.I.; Fernandes, C. A Meta-Model to Predict the Drag Coefficient of a Particle Translating in Viscoelastic Fluids: A Machine Learning Approach. *Polymers* **2022**, *14*, 430. [CrossRef] [PubMed]
99. Aziz, A.; Driouich, A.; Bellil, A.; Ben Ali, M.; Mabtouti, S.E.; Felaous, K.; Achab, M.; El Bouari, A. Optimization of new eco-material synthesis obtained by phosphoric acid attack of natural Moroccan pozzolan using Box-Behnken Design. *Ceram. Int.* **2021**, *47*, 33028–33038. [CrossRef]
100. Cesari, M.; Stefani, A.; Mitterling, T.; Frauscher, B.; Schönwald, S.V.; Högl, B. Sleep modelled as a continuous and dynamic process predicts healthy ageing better than traditional sleep scoring. *Sleep Med.* **2021**, *77*, 136–146. [CrossRef]
101. Qadir, Z.; Khan, S.I.; Khalaji, E.; Munawar, H.S.; Al-Turjman, F.; Mahmud, M.P.; Kouzani, A.Z.; Le, K. Predicting the energy output of hybrid PV–wind renewable energy system using feature selection technique for smart grids. *Energy Rep.* **2021**, *7*, 8465–8475. [CrossRef]
102. Sallehhudin, W.; Diab, A. Using Machine Learning to Predict the Fuel Peak Cladding Temperature for a Large Break Loss of Coolant Accident. *Front. Energy Res.* **2021**, *9*, 755638. [CrossRef]
103. Ahmadi, K.; Alavi, S.J.; Kouchaksaraei, M.T.; Aertsen, W. Non-linear height-diameter models for oriental beech (*Fagus ori-entalis* Lipsky) in the Hyrcanian forests, Iran. *Biotechnol. Agron. Soc. Environ.* **2013**, *17*, 431–440.

104. Oussama, C.; Abdellah, E.A.; Youssef, E.O.; Mohammed, B.; Abdelkrim, O. In silico Prediction of Novel SARS-CoV 3CL pro Inhibitors: A Combination of 3D-QSAR, Molecular Docking, ADMET Prediction, and Molecular Dynamics Simulation. *Biointerface Res. Appl. Chem.* **2022**, *12*, 5100–5115. [CrossRef]
105. Gramatica, P. On the Development and Validation of QSAR Models. *Methods Mol. Biol.* **2013**, *930*, 499–526. [CrossRef] [PubMed]
106. Gohain, P.B.; Jansson, M. Scale-Invariant and consistent Bayesian information criterion for order selection in linear regression models. *Signal Process.* **2022**, *196*, 108499. [CrossRef]
107. Banteng, L.; Yang, H.; Chen, Q.; Wang, Z. Research on the subtractive clustering algorithm for mobile ad hoc network based on the Akaike information criterion. *Int. J. Distrib. Sens. Netw.* **2019**, *15*, 1550147719877612. [CrossRef]
108. Banks, H.T.; Joyner, M.L. Adaption of Akaike information criterion under least squares frameworks for comparison of stochastic models. *Q. Appl. Math.* **2019**, *77*, 831–859. [CrossRef]
109. Tozzi, R.; Masci, F.; Pezzopane, M. A stress test to evaluate the usefulness of Akaike information criterion in short-term earthquake prediction. *Sci. Rep.* **2020**, *10*, 21153. [CrossRef]
110. Benedet, A.L.; Brum, W.S.; Hansson, O.; Karikari, T.K.; Zimmer, E.R.; Zetterberg, H.; Blennow, K.; Ashton, N.J. Alzheimer's Disease Neuroimaging Initiative the accuracy and robustness of plasma biomarker models for amyloid PET positivity. *Alzheimer's Res. Ther.* **2022**, *14*, 26. [CrossRef]
111. Bhattacharya, S.; Biswas, A.; Nandi, S.; Patra, S.K. Exhaustive model selection in b$\to$s$\ell\ell$ decays: Pitting cross-validation against the Akaike information criterion. *Phys. Rev. D* **2020**, *101*, 055025. [CrossRef]
112. Pham, H. A New Criterion for Model Selection. *Mathematics* **2019**, *7*, 1215. [CrossRef]
113. Tran, D.A.; Tsujimura, M.; Ha, N.T.; Nguyen, V.T.; van Binh, D.; Dang, T.D.; Doan, Q.-V.; Bui, D.T.; Ngoc, T.A.; Phu, L.V.; et al. Evaluating the predictive power of different machine learning algorithms for groundwater salinity prediction of multi-layer coastal aquifers in the Mekong Delta, Vietnam. *Ecol. Indic.* **2021**, *127*, 107790. [CrossRef]
114. Saez, L.M.A.; Campos, F.M.A.; Callejón-Ferre, J.; Medina, M.D.S.; Fernández, I. Use of multivariate NMR analysis in the content prediction of hemicellulose, cellulose and lignin in greenhouse crop residues. *Phytochemistry* **2019**, *158*, 110–119. [CrossRef]
115. Ezuma, M.; Anjinappa, C.K.; Funderburk, M.; Guvenc, I. Radar Cross Section Based Statistical Recognition of UAVs at Microwave Frequencies. *IEEE Trans. Aerosp. Electron. Syst.* **2022**, *58*, 27–46. [CrossRef]
116. Ikbal, N.A.M.; Halim, S.A.; Ali, N. Estimating Weibull Parameters Using Maximum Likelihood Estimation and Ordinary Least Squares: Simulation Study and Application on Meteorological Data. *Math. Stat.* **2022**, *10*, 269–292. [CrossRef]
117. Xu, Q.; Li, R.; Liu, Y.; Luo, C.; Xu, A.; Xue, F.; Xu, Q.; Li, X. Forecasting the Incidence of Mumps in Zibo City Based on a SARIMA Model. *Int. J. Environ. Res. Public Health* **2017**, *14*, 925. [CrossRef]
118. Tikhonov, A.N. On the solution of ill-posed problems and the method of regularization. In *Doklady Akademii Nauk*; Russian Academy of Sciences: Moscow, Russia, 1963; pp. 501–504. [CrossRef]
119. Calvetti, D.; Morigi, S.; Reichel, L.; Sgallari, F. Tikhonov regularization and the L-curve for large discrete ill-posed problems. *J. Comput. Appl. Math.* **2000**, *123*, 423–446. [CrossRef]
120. Rasmussen, C.E.; Williams, C.K.I. *Gaussian Processes for Machine Learning*; the MIT Press: Cambridge, MA, USA, 2006; ISBN 026218253X.
121. Wolfe, P. Convergence Conditions for Ascent Methods. *SIAM Rev.* **1969**, *11*, 226–235. [CrossRef]
122. Wolfe, P. Convergence Conditions for Ascent Methods. II: Some Corrections. *SIAM Rev.* **1971**, *13*, 185–188. [CrossRef]